# The Effects of Eccentricity in Central Plate of Concentrically Braced Frames

**M. Bastami**
*Assistant Professor, International Institute of Earthquake Engineering and Seismology (IIEES), Tehran, Iran & Assistant Professor, University of Kurdistan, Sanandaj, Iran (m.bastami@iiees.ac.ir, m.bastami@uok.ac.ir)*

**M.S. Abdi**
*Department of Civil Engineering, University of Kurdistan, Sanandaj, Iran & Faculty of Civil Department, Islamic Azad University, Marivan, Iran (shahrokhabdi65@gmail.com)*

**SUMMARY**
Buckling of conventional braces in concentrically braced frames (CBFs), caused limitation of ductility and energy dissipation of lateral resistance force systems. In order to improve ductility of CBFs by adding eccentricity in the central plate of CBFs, ductility and stiffness of these braced frames named ECBFs, studied. Three types of single degree freedom systems with span length to frame height ratio (L/H) equal to 0.67, 1.00 and 1.33 was studied. Also multi degree freedom of this system with and without change in plate thickness and plate eccentricity in height of structure modeled. The results show that the frame's shear stiffness and energy absorption increase by raising (L/H) ratio. Increasing plate thickness caused energy absorbing of system to rise from 2.80 to 11.20 times. This also led to increasing energy absorption in MDOF from 2.57 to 6.78 times.

*Keywords: Ductility, Energy absorption, Bracing frame, CBF, EBF*

## 1. INTRODUCTION

Steel frame structural systems have been widely used in the worldwide for mid to high rise structures. A large majority of these systems built before 1994 consisted of steel moment resisting frames to provide lateral resistance during an earthquake. The occurrence of the 1994 Northridge earthquake and 1995 Hyogoken–Nanbu (Kobe) earthquake caused unexpected damage to many of these systems due to the fracture of welded beam to column connections resulting in unacceptably large lateral displacements [Nakashima et al. 1998]. In order to prevent future problems associated with geometric nonlinearities and brittle fracture of the beam–column connection in steel moment-resisting frames, research in the United States has focused on understanding the nonlinear and brittle performance of these steel frame structures. Significant efforts were undertaken to develop different connection geometries and configurations to mitigate these problems [Nakashima et al. 2000]. The problems associated with steel moment-frame systems also led to a search for alternative economical lateral load resisting systems, such as the use of concentrically braced frames, and more recently special concentrically braced frames [Sabol 2004]. Concentrically braced frames (CBFs) continue to be used as lateral load resisting systems with expected increases in their use as new systems and design approaches are developed. Although there has been an increase in the use of braced frame systems, but damage during past earthquakes suggests that braced systems may perform poorly due to limited ductility and energy dissipation of the bracing system, failure of the connection between the braces and the frame, and asymmetric behavior of the brace in tension and compression [Sabelli et al. 2003]. A lack of knowledge in regards to the behavior of concentrically braced steel frame systems has prompted efforts to characterize the performance of such structures and develop more reliable design standards [McCormic et al. 2007]. Hysteretic behavior of CBFs, as a system, highly depends on the hysteretic behavior of bracing members. Hysteretic loops of an axially loaded brace subject to buckling are usually unsymmetrical with degradation of the buckling strength and hysteretic energy dissipation in compression in each subsequent cycle [Celik et al. 2006].

In spite of noticeable disadvantages, some defects of CBF system caused more research to be accomplished. In 1990, ductile bracing liken was proposed and then many various tests were performed in USA and Japan. In these systems enclosed area between loops in stress-strain curve due to yielding the bracing member, explained the amount of dissipated energy [Baz Havaei and Zahrai 2008]. Yielding damped bracing frames (YDBF) which work on the basis of material yielding and pose in the crossing of two convergent bracings, build a closed frame with four connected edges to CBF arms. Material of this central system, which is an energy absorber is built from the flexible steel and is designed to yield in serious and medium earthquake shakes [Roufegarinejad and Sabouri 2002]. In 1998 Jurukovski and Simenov worked on these systems as inventors of yielding damped bracing frames by hollow (cylindrical) cross section which is filled by concrete. The prepared nonlinear dynamic analysis of these systems and the result was compared with a full scale model and tested in laboratory [Jurukovski and Simenov 1988]. Ciampi and Ferreti have studied these systems and offered two different YDBF [Ciampi and Ferreti 1990]. Vulcano has worked on Pall and Marsh and also YDBF [Vulcano 1995]. He continued Ciampi's studies. In 2002 Roufegarinejad and Sabouri proposed the method of modeling and optimizing dimensions of interior YDBF member, besides introducing this system [Roufegarinejad and Sabouri 2002].

Ideally, from the perspective of seismic design, it is desirable to delay (or possibly prevent) global and local buckling of braces in steel frames [Iwata et al., 2000]. To improve the hysteretic characteristics of CBFs, we considered an eccentricity in middle gusset plate. The gusset plate shall not be so thick to guarantee its shear yielding performance. Therefore, by designing braces that do not buckle in cyclic loading, the gusset plate can perform inelastic hysteretic response. This new system is named ECBF (Eccentricity in concentrically braced frame).

Fig. 1 shows a schematic one-story frame that has a rectangular internal frame at intersection of braces. In fact, the internal frame performs as seismic energy damper designed for moderate and high level earthquakes. Suitable behavior in tension, compression and high capability in energy dissipation of Yielding Damped Braced Frame (YDBF) are noticeable. Unlike YDBF, ECBF do not have a middle frame but have eccentricity in the middle gusset plate. In YDBF, the deformation is concentrated in connections, while in ECBF, this role is postponed to the gusset plate that indicates a special performance of the braced frame in the compression and tension active therefore there is not any change in the hysteresis loops.

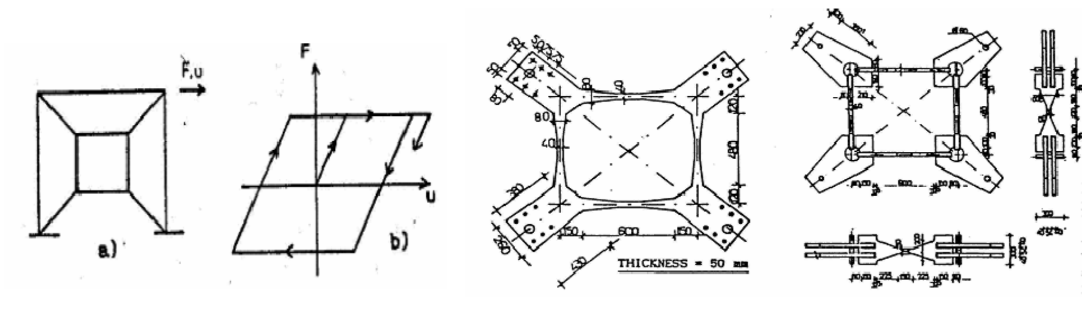


**Figure 1.** Central Yielding Damper with Simple and Rigid Connection to Braces [Jurukovski et al. 2000]

## 2. METHODOLOGY FOR DESIGN ECBFs

Three types of single degree of freedom (SDOF) models for ECBFs with three ratios of span length to frame height$\left(\frac{L}{H}\right)$, including 0.67, 1.00 and 1.33 are modeled (see Table 1). For the each ratio, there are 35 models categorized in 7 groups with 2, 5, 10, 15, 20, 25 and 30 percent of eccentricity in the middle gusset plate. Also each group has 5 sub-groups with different gusset plate thickness. In addition, 18 models of ECBF in multi degree of freedom (MDOF) including one span and three stories with $\left(\frac{L}{H}\right)$ ratio equal to 1.33 are also considered (see Table 2).

To design an ECBF, at first, yielding force and then ultimate force of the gusset plate is calculated. In proportion to the ultimate force, maximum design force of the model members shall be calculated. To achieve the maximum force for design each model, relationships 1 to 10 are applied. These relationships are presented for two statues of plate, one before plate buckling, and the other for post buckling [Sabouri 2001]:

- Pre plate buckling: In this case, critical shear stress in the plate, $\tau_{cr}$, could be obtained as equation (1):

$$\tau_{cr} = \frac{K\pi^2 E}{12(1-\mu^2)}\left(\frac{t}{b}\right)^2 \quad (1)$$

$$F_{cr} = \tau_{cr} bt \quad (2)$$

$$F_u = 1.4F_{cr} \quad (3)$$

In the above formulas, $\tau_{cr}$ is critical shear stress in the plate, K is a factor calculated by below relationships:

$$K = 5.35 + 4\left(\frac{b}{d}\right)^2 \qquad \frac{d}{b} \geq 1 \quad (4)$$

$$K = 5.35\left(\frac{b}{d}\right)^2 + 4 \qquad \frac{d}{b} \leq 1 \quad (5)$$

- Post plate buckling:

$$\sigma_{xy} = \sigma_{yx} = \tau_{cr} + \frac{1}{2}\sigma_{ty}\sin 2\theta \quad (6)$$

$$3\tau_{cr}^2 + 3\tau_{cr}\sigma_{ty}\sin 2\theta + \sigma_{ty}^2 - \sigma_0^2 = 0 \quad (7)$$

$$F_{wu} = \sigma_{xy} bt = bt\left(\tau_{cr} + \frac{1}{2}\sigma_{ty}\sin 2\theta\right) \quad (8)$$

$$F_u = 1.4F_{wu} \quad (9)$$

*b* is plate length in beam direction, d is plate length in column direction, t is plate thickness, θ is angle of struts replacing a gusset plate, $\sigma_{ty}$ is stress in tension field action and $\sigma_0$ is steel yielding stress.

Finally, for calculating maximum force for design of each model, the ultimate force increased by a constant factor equal to 2.86 resulting from many trial and error analyses of various models of ECBFs to gain a factor to increase design force so the braces do not buckle that indicates the gusset plate play main role to improve ductility and energy absorption of ECBFs. Therefore maximum force can be obtained by below formula:

$$F_{max} = 2.86\mathrm{F_u} \quad (10)$$

Results of designing the ECBF models are mentioned in Tables 1 and 2.

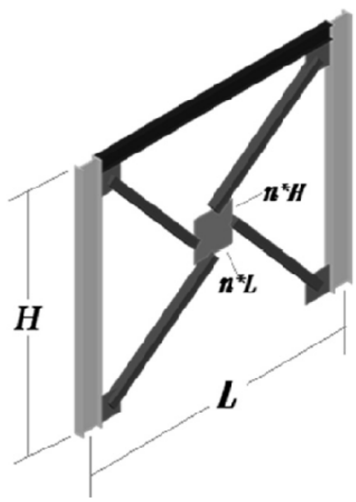


**Figure 2.** Schematic model of ECBF

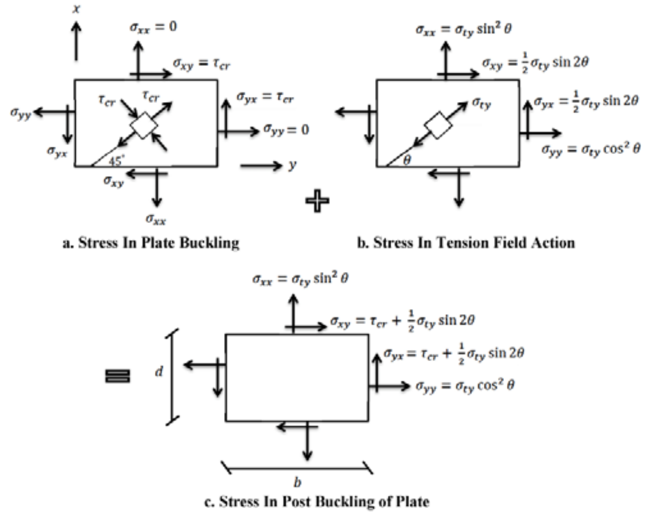


**Figure 3.** Stress in plate before and after buckling [Sabouri 2001]

## 3. PUSHOVER ANALYSIS OF ECBFs

A pushover analysis is basically a step-by-step plastic analysis for which the lateral loads of constant relative magnitude are applied to a given structure and progressively increased until a target displacement is reached, while gravity loads are kept constant. Thus, as the name implies, the structure is truly pushed sideway to determine its ultimate lateral-load resistance as well as the sequence of yielding events needed to reach that goal, or the magnitude of plastic deformations at the target displacement [Bruneau 1998].

In this study, to achieve capacity curve of ECBF models, in SDOF system, a single point load was applied in roof of the models and increased until target displacements was reached. However in MDOF models, a triangle load can be applied. In this type of loading, 100% of the load applies in roof story and for other stories, decrease until reaching zero at the base of structure. Some of the capacity curves are presented in Figures 4 and 5.

Results show that for a constant plate eccentricity, increasing plate thickness will increase ECBFs stiffness. Also, the maximum displacement and the maximum shear force that a MDOF model of ECBFs can resist, enlarge by increasing plate thickness and plate eccentricity (Figures 6 and 7).

Regards to the results, increasing plate size, for a constant thickness, caused an increase in roof displacement of ECBFs. Moreover, this increase is added by increasing $\left(\frac{L}{H}\right)$ ratio. However, Fig. 8 indicates that an eccentricity of about 10-20% is appropriate to obtain a maximum lateral stiffness for ECBFs. By using the pushover analysis results, the response and ductility factor of ECBF models (at SDOF or MDOF) can be calculated. These results are summarized in Tables 3 for both SDOF and MDOF. Furthermore, the average results for the response factor of ECBF models (in SDOF or MDOF) are shown in Table 4.

**Table 1.** Some of SDOF models of ECBF

| Model Name | Beam Length (mm) | Column Length (mm) | Eccentricity or n(%) | b (mm) | d (mm) | t (mm) | Beam Section | Column Section | Braces Section |
|---|---|---|---|---|---|---|---|---|---|
| ECBF-1-1-T1 | 2000 | 3000 | 2 | 40 | 60 | 0.14 | IPE14 | IPE14 | HSS 60*60*4 |
| ECBF-1-2-T2 | 2000 | 3000 | 5 | 100 | 150 | 0.72 | IPE14 | IPE18 | HSS 60*60*4 |
| ECBF-1-3-T1 | 2000 | 3000 | 10 | 200 | 300 | 0.72 | IPE14 | IPE20 | HSS 60*60*8 |
| ECBF-1-4-T4 | 2000 | 3000 | 15 | 300 | 450 | 4.89 | IPE14 | IPE45 | HSS 140*140*25 |
| ECBF-1-5-T2 | 2000 | 3000 | 20 | 400 | 600 | 2.87 | IPE14 | IPE36 | HSS 140*140*20 |
| ECBF-2-1-T2 | 3000 | 3000 | 2 | 60.00 | 60.00 | 0.38 | IPE18 | IPE16 | HSS 60*60*4 |
| ECBF-2-2-T2 | 3000 | 3000 | 5 | 150.00 | 150.00 | 0.94 | IPE18 | IPE18 | HSS 60*60*8 |
| ECBF-2-3-T1 | 3000 | 3000 | 10 | 300.00 | 300.00 | 0.94 | IPE18 | IPE22 | HSS 70*70*8 |
| ECBF-2-4-T2 | 3000 | 3000 | 15 | 450.00 | 450.00 | 2.82 | IPE18 | IPE45 | HSS 120*120*20 |
| ECBF-3-1-T5 | 4000 | 3000 | 2 | 80.00 | 60.00 | 1.26 | IPE24 | IPE18 | HSS 60*60*4 |
| ECBF-3-2-T4 | 4000 | 3000 | 5 | 200.00 | 150.00 | 2.37 | IPE24 | IPE30 | HSS 90*90*10 |
| ECBF-3-3-T3 | 4000 | 3000 | 10 | 400.00 | 300.00 | 3.16 | IPE24 | IPE50 | HSS 120*120*20 |
| ECBF-3-4-T1 | 4000 | 3000 | 15 | 600.00 | 450.00 | 1.56 | IPE24 | IPE40 | HSS 100*100*16 |

**Table 2.** Some of MDOF models of ECBF with$\left(\frac{L}{H} = 1.33\right)$

| Model Name | Story | Beam Length (mm) | Column Length (mm) | Eccentricity or n(%) | b (mm) | d (mm) | t (mm) | Beam Section | Column Section | Braces Section |
|---|---|---|---|---|---|---|---|---|---|---|
| ECBF-M-1 | Third | 4000 | 3000 | 5 | 200.00 | 150.00 | 1.00 | IPE24 | HSS 80*80*8 | HSS 60*60*10 |
| | Second | 4000 | 3000 | 5 | 200.00 | 150.00 | 2.00 | IPE24 | HSS 90*90*16 | HSS 80*80*10 |
| | First | 4000 | 3000 | 5 | 200.00 | 150.00 | 3.00 | IPE24 | HSS 120*120*16 | HSS 90*90*16 |
| ECBF-M-8 | Third | 4000 | 3000 | 10 | 400.00 | 300.00 | 4.00 | IPE24 | HSS 160*160*25 | HSS 140*140*20 |
| | Second | 4000 | 3000 | 10 | 400.00 | 300.00 | 8.00 | IPE24 | HSS 220*220*35 | HSS 180*180*30 |
| | First | 4000 | 3000 | 10 | 400.00 | 300.00 | 12.00 | IPE24 | HSS 260*260*40 | HSS 220*220*35 |
| ECBF-M-12 | Third | 4000 | 3000 | 15 | 600.00 | 450.00 | 4.00 | IPE24 | HSS 180*180*30 | HSS 160*160*25 |
| | Second | 4000 | 3000 | 15 | 600.00 | 450.00 | 8.00 | IPE24 | HSS 260*260*40 | HSS 220*220*35 |
| | First | 4000 | 3000 | 15 | 600.00 | 450.00 | 12.00 | IPE24 | HSS 360*360*40 | HSS 280*280*40 |
| ECBF-M-18 | Third | 4000 | 3000 | 5 | 200.00 | 150.00 | 12.00 | IPE24 | HSS 180*180*30 | HSS 160*160*25 |
| | Second | 4000 | 3000 | 10 | 400.00 | 300.00 | 12.00 | IPE24 | HSS 260*260*40 | HSS 220*220*35 |
| | First | 4000 | 3000 | 15 | 600.00 | 450.00 | 12.00 | IPE24 | HSS 360*360*40 | HSS 280*280*40 |

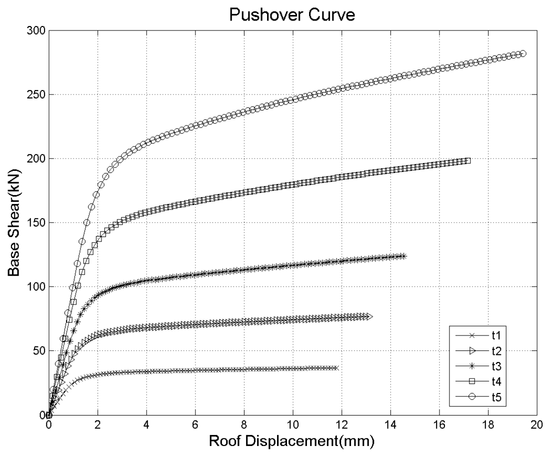


**Figure 4.** Comparison of capacity curve of ECBF-1-4-T1 to ECBF-1-4-T5 models

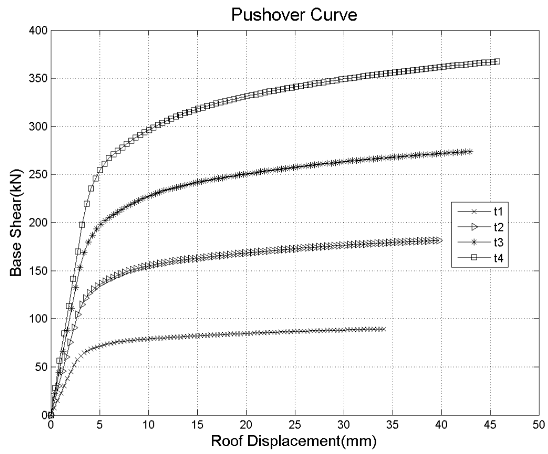


**Figure 5.** Comparison of capacity curve of ECBF-M-5 to ECBF-M-8 models

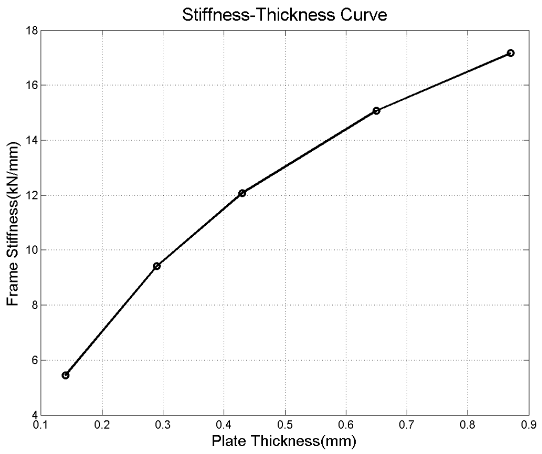


**Figure 6.** Variations of ECBF-1-1 stiffness vs. gusset plate thickness

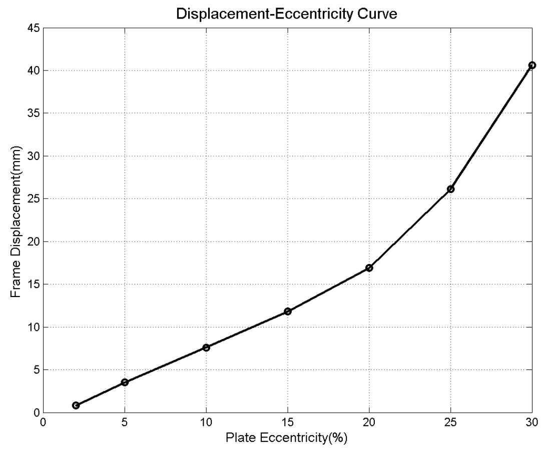


**Figure 7.** Variations of ECBF-1 roof displacement vs. plate eccentricity in SDOF state

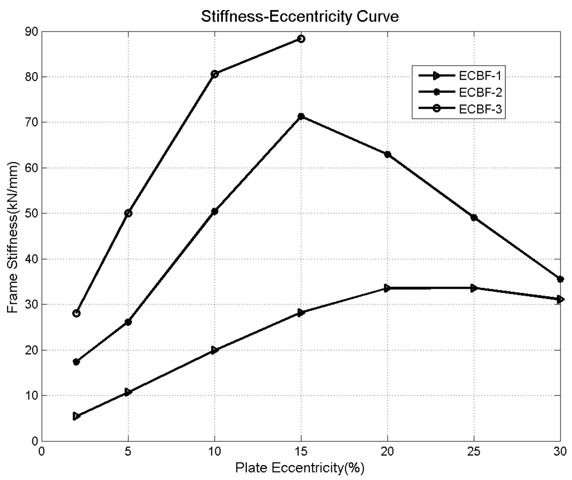


**Figure 8.** The effects of $\left(\frac{L}{H}\right)$ ratio and plate eccentricity on ECBF stiffness in SDOF state

**Table 3.** Response and ductility factor of ECBF models in SDOF

| Model Name | Model's Period (s) | $R_\mu$ | $R = Y \times \Omega_0 \times R_\mu$ |
|---|---|---|---|
| ECBF-3-2-T3 | 0.14 | 4.51 | 9.25 |
| ECBF-3-2-T4 | 0.12 | 4.52 | 9.26 |
| ECBF-3-2-T5 | 0.11 | 4.71 | 9.06 |
| ECBF-3-3-T1 | 0.15 | 4.61 | 9.20 |
| ECBF-3-3-T2 | 0.12 | 4.58 | 9.25 |
| ECBF-3-3-T3 | 0.10 | 4.51 | 9.55 |
| ECBF-M-11 | 0.32 | 4.64 | 8.65 |
| ECBF-M-12 | 0.29 | 4.70 | 8.78 |
| ECBF-M-7 | 0.34 | 4.78 | 8.93 |
| ECBF-M-8 | 0.31 | 4.71 | 8.80 |
| ECBF-M-9 | 0.49 | 4.59 | 8.57 |
| ECBF-M-10 | 0.37 | 4.65 | 8.67 |
| ECBF-M-11 | 0.32 | 4.64 | 8.65 |

**Table 4.** ECBF average response factor

| Model Name | $R_\mu$ | Average of $\mathbf{R}_\mu$ | $R = Y \times \Omega_0 \times R_\mu$ | Average of R |
|---|---|---|---|---|
| ECBF-1 (SDOF) | 4.50 | | 9.85 | |
| ECBF-2 (SDOF) | 4.53 | 4.53 | 9.47 | 9.53 |
| ECBF-3 (SDOF) | 4.57 | | 9.28 | |
| ECBF (MDOF) | 4.63 | 4.63 | 8.66 | 8.66 |

## 4. CYCLIC PUSHOVER ANALYSIS OF ECBFs

Cyclic pushover analysis is useful to detection the cyclic inelastic behavior of structures, particularly when the intent is to investigate the impact of the unidirectional energy dissipation mechanisms on structural responses. To do these analyses, the cyclic displacement history shown in Fig. 9, is used.
Working step by step through the applied cyclic displacement history, one observed that for a constant eccentricity, increasing plate thickness increases energy absorption by average of 2.80 to 11.20 times. Also results show that energy absorption of the models with $(\mathrm{L/H} = 1.0)$ and $(\mathrm{L/H} = 1.33)$ are 4.62 and 9.44 times of the models by $(\mathrm{L/H} = 1.33)$ respectively. Therefore, increasing of $(L/H)$ ratio can increase energy absorption. Results of MDOF models, also show that increasing plate eccentricity and plate thickness can increase energy absorption from 2.57 to 6.78 times.

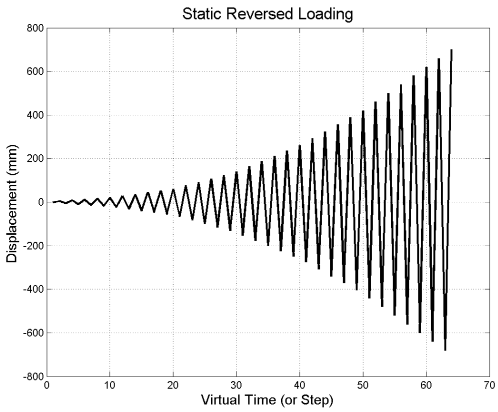


**Figure 9.** Cyclic displacement history in cyclic pushover analysis

Figs. 10 to 12 present energy absorption in SDOF of ECBF models for $\left(\frac{\mathrm{L}}{\mathrm{H}} = 0.67, 1.00, 1.33\right)$ in eccentricity equal to 5%. Also Fig. 13 shows a comparison of energy absorption in the ECBFs vs. eccentricity in the gusset plate for different $(L/H)$ ratio of the frames. This show that in all $(\mathrm{L/H})$ ratios, increasing eccentricity causes that energy absorption decreased.

## 5. COMPARISION BETWEEN CBF, CBF AND EBF

To compare seismic behavior of ECBF with EBF and CBF systems, the same shear forces are used to design EBFs and CBFs. The both previous analyses, i.e. pushover analysis and cyclic pushover analysis, are performed to detect seismic behavior of EBF and CBF models. Results show that by increasing the eccentricity and thickness, the energy absorption of ECBFs increased that in most cases is more than that of CBFs. Results show that on average, energy absorption of ECBF is 1.43 times that of CBFs and 0.79 times that of EBFs. Fig. 14 compares the energy absorbed in some of the ECBF, CBF and EBF models. Figs. 15 and 16 show comparisons between ECBF and EBF and CBF stiffness in SDOF and MDOF. Results illustrate that stiffness of ECBF in SDOF, for $(L/H)$ ratio of 0.67, 1.00 and 1.33, is greater than CBF models by 27%, 77% and 77% and, in comparison with EBF models, is greater by 91%, 100% and 92% respectively. Also as MDOF, stiffness of ECBF system is greater than stiffness of CBF and EBF systems in all models.

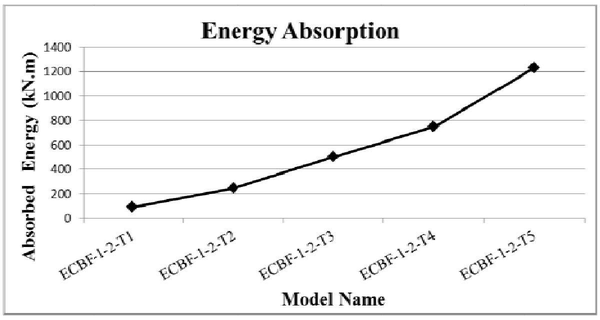


**Figure 10.** Energy absorption of ECBFs by 5% eccentricity with $\left(\frac{L}{H} = 0.67\right)$

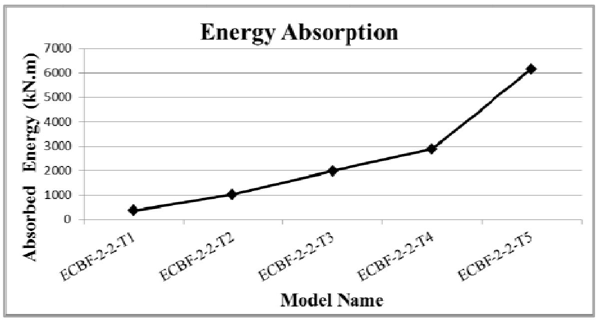


**Figure 11.** Energy absorption of ECBFs by 5% eccentricity with $\left(\frac{L}{H} = 1.00\right)$

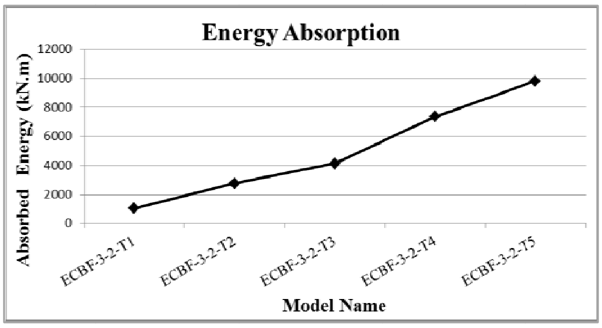


**Figure 12.** Energy absorption of ECBFs by 5% eccentricity with $\left(\frac{L}{H} = 1.33\right)$

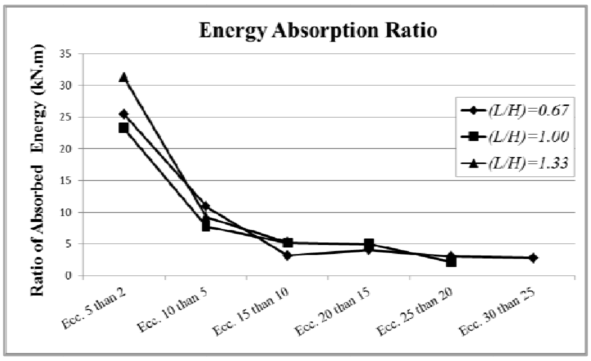


**Figure 13.** Comparison of energy absorption in plate eccentricity increasing for different $\left(\frac{L}{H}\right)$ ratio

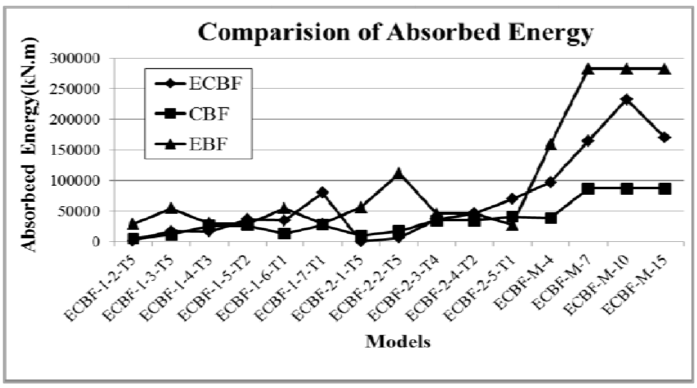


**Figure 14.** Comparison between absorbed energy in some of ECBF, CBF and EBF models

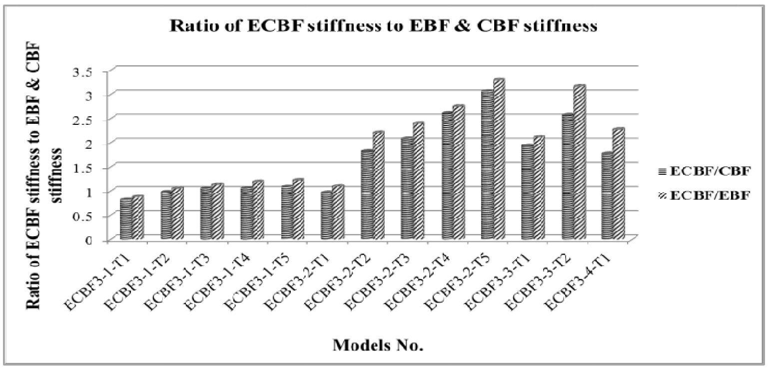


**Figure 15.** Comparison between ECBF stiffness with EBF and CBF for $\left(\frac{L}{H} = 1.33\right)$ in SDOF

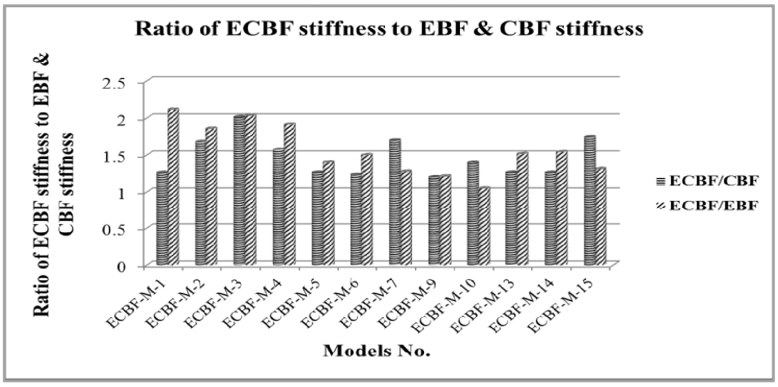


**Figure 16.** Comparison between ECBF stiffness with EBF and CBF for $\left(\frac{L}{H} = 1.33\right)$ in MDOF

## 6. CONCLUSIONS

In order to improve ductility and energy absorption of CBFs, an eccentricity is added in connection of the braces and the middle gusset plate, which are named ECBFs. The goal of this system is that the bulk of yielding, energy dissipation and damage in the system will occur in the middle gusset plate itself not in other members. Energy dissipation mechanism of the system is shear yielding of the gusset plate. In this study, the effects of eccentricity in the central plate of CBFs are examined. The system, designed and detailed properly, not only is very ductile and has relatively large energy dissipation capability, but also has relatively high stiffness, thus is very effective in limiting the drift and energy absorbing. Results show that increasing both plate thickness and plate eccentricity can increase frame stiffness. Also increasing frame span to frame height ratio, will increase energy absorption of these frames. Increasing plate thickness in SDOF caused energy absorption of system to rise from 2.80 to 11.20 times, but increasing plate eccentricity caused frame stiffness first to increase until it's eccentricity reach 15%; then the frame's stiffness decreased with increasing plate eccentricity. Also, this can increase energy absorption in MDOF from 2.57 to 6.78 times. The response factor of ECBF as SDOF and MDOF are calculated 9.53 and 8.66, respectively. Compared with eccentrically braced frames (EBF) and concentrically braced frames (CBF), the ECBF is stiffer than both EBF and CBF models by 27%, 77%, 77% and 91%, 100%, 92% for $\left(\frac{L}{H}\right) = 0.67, 1.00\ and\ 1.33$, respectively. In MDOF models, all ECBF models are stiffer than both EBF and CBF systems; although results showed that energy absorption of ECBF is 1.43 and 0.79 times that of CBF and EBF, respectively.

**References**


Baz Havaei, G., Zahraei, M. (2008) "Impact of number of stories on seismic behavior of yielding damped braced frames", *4th national congress on civil engineering*, Iran.

Bruneau, M., Whittaker, A.S., and Uang, C.M. (1998). "Ductile Design of Steel Structures", *McGraw-Hill*, NY.

Celik, O. C., Berman, J. W., and Bruneau, M. (2006). "Hysteretic energy dissipation in laterally restrained steel tube and solid bar braces", *First European Conference on Earthquake Engineering and Seismology*, Geneva, Switzerland.

Ciampi, V. and Ferretti, S.A., (1990) "Energy dissipation in buildings using special bracing systems", *Proceeding of 10th Earthquake Conf.*

Iwata, M., Kato, T. and Wada, A. (2000), "Buckling-Restrained Braces as Hysteretic Dampers", *3rd International Conference on Behavior of Steel Structures in Seismic Areas (STESSA 2000)*, Montreal, Canada, 33-38.

Jurukovski D., Petkovski M. and Rakicevic Z. (2000) "Energy absorbing in regular and composite steel frame structures" *Engineering Structures* , Vol .17, 314 –333.

Jurukovski, Dimitar; Simenov, Boris (1988) "Effectiveness of energy absorbing elements in composite steel frame structures", *Nine world conference on earthquake engineering*, Japan.

McCormic, J., DesRoches, R., Fugazza, D., Auricchio, F. (2007). "Seismic assessment of concentrically braced steel frames with shape memory alloy braces" *J. Struct. Eng.*, 133(6), 862–870.

Nakashima, M., Inoue, K., and Tada, M. (1998). "Classification of damage to steel buildings observed in the 1995 Hyogoken-Nanbu Earthquake" *Eng. Struct.*, 20(4–6), 271–281.

Nakashima, M., Roeder, C. W., and Maruoka, Y. (2000). "Steel moment frames for earthquakes in United States and Japan" *J. Struct. Eng.*, 126(8), 861–868.

Roufegarinejad, A and Sabouri, S. (2002) "Nonlinear behavior of yielding damped bracing frames", *15th ASCE Engineering Mechanics Conference*, Columbia University, New York, NY.

Sabelli, R., Mahin, S., and Chang, C. (2003). "Seismic demands on steel braced frame buildings with buckling-restrained braces" *Eng. Struct.*, 25(5), 655–666.

Sabol, T. A. (2004). "An assessment of seismic design practice of steel structures in the United States since the Northridge Earthquake" *Struct. Des. Tall Build.*, 13(5), 409–423.

Sabouri, S. (2001) "Load resisting systems an introduction to steel shear walls (SSW)", *Anguizeh Publishing Co.*

Vulcano, A., (1995) "Design of damped steel bracing systems for seismic control of framed structures", *10th European Conference on Earthquake Engineering*, Duma(ed.), 1567-1572.